Biodegradation of vulcanized rubber by a gut bacterium from plastic-eating mealworms

3 authors, including:

Yu Yang

Beijing Institute of Technology

24 PUBLICATIONS   **1,949** CITATIONS

SEE PROFILE

Research Paper

Biodegradation of vulcanized rubber by a gut bacterium from plastic-eating mealworms

Xiaotao Cheng, Mengli Xia, Yu Yang [*,1]

Department of Biology, School of Life Science, Beijing Institute of Technology, Beijing 100081, PR China

HIGHLIGHTS

- A bacterium *Acinetobacter* sp. BIT-H3 isolated from mealworm' gut can grow on and degrade vPR.
- Strain BIT-H3 can break down both sulfide bridges and polymeric backbone within vPR.
- Sulfate and oligo(*cis*-1,4 isoprene) with terminal aldehyde and keto were released from vPR degradation.
- The dszA, dszC1, dszC2, Laccase2147, and Peroxidase1232 were responsible for vPR degradation.

GRAPHICAL ABSTRACT
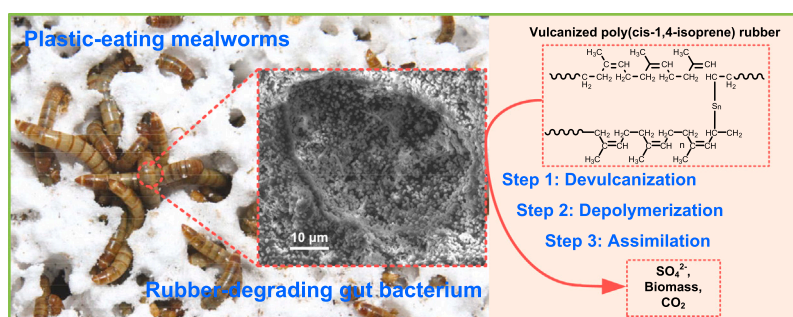
ARTICLE INFO

ABSTRACT

The disposal of vulcanized rubber waste is difficult due to the presence of three-dimensional crosslinking network structure. Here, we report that a bacterium *Acinetobacter* sp. BIT-H3, isolated from the gut of plastic-eating mealworm, can grow on and degrade vulcanized poly(cis-1,4-isoprene) rubber (vPR). Scanning electronic microscopy (SEM) shows that strain BIT-H3 can penetrate into the vPR and produce craters and cracks. The tensile strength and the crosslink density of vPR decreased by 53.2% and 29.3% after ten weeks' incubation, respectively. The results of Horikx analysis, attenuated total reflectance-Fourier transform infrared (ATR-FTIR) spectroscopy, and X-ray absorption near-edge structure (XANES) spectroscopy reveal that strain BIT-H3 can break down both sulfide bridges and double bonds of polymeric backbone within vPR. Sulfate and oligo(*cis*-1,4 isoprene) with terminal aldehyde and keto groups were identified as metabolic products released during vPR degradation. Through genomic and transcriptional analyses, five enzymes of dszA, dszC1, dszC2, Laccase2147, and Peroxidase1232 were found to be responsible for vPR degradation. Based on the chemical structure characterizations and molecular analyses, a vPR biodegradation pathway was proposed for strain BIT-H3. These findings pave a way for exploiting vulcanized rubber-degrading microorganisms from insect gut and contribute to establish a biodegradation method for vulcanized rubber waste disposal.

* Correspondence to: Department of Biology, School of Life Science, Beijing Institute of Technology, 5 South Zhongguancun Street, Beijing 100081, PR China.
E-mail address: yooyoung@bit.edu.cn (Y. Yang).
[1] ORCID: 0000-0002-4663-9753.

Environmental Implication

Vulcanized rubber waste is durable due to the cross-linked network structure and could cause significant environment pollution, such as spontaneous combustion, releasing microparticles, and as vector transmitting pollutants and pathogens. This work firstly reports a bacterium *Acinetobacter* sp. BIT-H3, isolated from the gut of plastic-eating mealworm, that can degrade vulcanized poly(cis-isoprene) rubber (vPR) by simultaneously cleaving both sulfide bridges and poly(cis-isoprene) backbone within the cross-linked network, and elucidates the vPR biodegradation mechanism by this strain. These findings pave a way for discovering vulcanized rubber-degrading microorganisms from insect gut and contribute to establish a biodegradation method for vulcanized rubber waste disposal.

Data availability

Data will be made available on request.

1. Introduction

Poly(cis-1,4-isoprene), consisting of many repeating units of —CH_2—$C(CH_3)$=CH—CH_2— in the *cis* configuration, is the main constituent of nature rubber. Usually, the linear poly(cis-1,4-isoprene) chains of nature rubber are covalently cross-linked by the sulfide bridges through a process of vulcanization, in order to improve the elasticity and durability of rubber products. Vulcanized poly(cis-1,4-isoprene) rubber (vPR) are widely applied in manufacturing two categories of products, of which 68% are vehicle tires and 42% are general rubber products, such as gloves, condoms, seals and so on [1]. Currently, the global consumptions of vPR has reached approximately 13.9 Mt/year [1]. Especially, in the past three years (2010–2022), the consumption of vPR products has increased drastically by about 10% due to a great demand of disposable medical gloves for the healthcare during the COVID-19 pandemic [2]. The increasing consumption of vPR products has inevitably generated huge amount of rubber waste. Once these rubber wastes are discarded into the nature, they would result in significant environment pollution, including spontaneous combustion [2], releasing microparticles [3], and as vector transmitting pollutants and pathogens [4]. Consequently, the disposal of vulcanized rubber waste has become a global environment concern.

The existing methods for rubber waste disposal mainly include landfilling, incineration, and reprocessing the rubber waste into powder for reusing [2]. Dumping rubber waste associated with municipal solid waste into landfilling is a simple way with low cost. However, the poor environmental degradability leads to the accumulation of rubber waste, which occupies a great amount of land area and leaches the toxic molecules into the local environment [1]. Incineration of rubber waste can reduce the volume of rubber waste and recover heat energy. But the released secondary pollutants, such as sulfur and nitrogen oxides, need to be treated, adding the cost burden for the operation [1]. As vulcanized rubber waste can't be melt and reshaped by heating process, the thermomechanical method generally used for plastic waste recycling is not suitable for rubber waste recycling. Currently, the only way for recycling rubber waste is to grind rubber waste into powders, which are subsequently applied as fillers for fabricating various composite materials. Prior to application, the rubber waste powders should be subjected to a modification process due to their poor interface compatibility with other materials. However, the present modification processes are considered to be unsustainable because they are greatly dependent on harsh chemicals, high temperature, and high pressure reaction conditions [1]. Therefore, it is urgent to explore a more sustainable and eco-friendly approaches for rubber waste disposal.

As an alternative, the application of specific microorganisms capable of degrading rubber for rubber waste disposal has garnered widespread interest, because of the advantages such as mild reaction conditions, low chemical and energy consumptions, and low discharge of secondary pollutants [5,6]. Nowadays, several sulfur-oxidizing bacteria (*Thiobacillus* spp.) or sulfur-reducing archaea (*Pyrococcus furiosus*) were reported to be able to selectively cleave the sulfide bridges (S-S and C-S bonds) but leave the polymeric backbones unbroken in vulcanized rubber [5]. This rubber desulfurization pathway is generally considered to be similar with the 4 S (sulfoxide/sulfone/sulfonate/sulfate) pathway which is catalyzed by the enzymes encoded with a *dsz* operon [5–7]. In addition, a number of Gram-positive bacteria (belong to the genera *Nocardia*, *Streptomyces*, *Gordonia*, *Rhodococcus*, and *Bacillus*), one Gram-negative bacterium (*Xanthomonas* sp. 35Y), and two fungi (*Trametes versicolor* and *Pleurotus ostreatus*) were found to be able to degrade non-vulcanized poly(cis-1,4-isoprene) rubber, by secreting rubber oxygenases (Lcp, RoxA, and RoxB), laccase, or peroxidase to cleave the double bonds of poly(cis-1,4-isoprene) chain [8–10]. However, it is so far unknown whether there are unique microorganisms that have the ability to simultaneously break down both sulfide bridges (S-S and C-S bonds) and poly(cis-1,4-isoprene) backbones within vPR. Our previous studies have demonstrated that mealworms, the insect larvae of *Tenebrio molitor* L., were able to eat and rapidly degrade Styrofoam [11]. The gut microbiota has been shown to play an important role in the plastic biodegradation and several plastic-degrading gut microorganisms have been isolated from the gut of mealworm [12–17]. Notably, it was also shown that mealworms could eat and degrade vulcanized styrene–butadiene rubber (v-SBR) by cleaving both sulfide bridges (S-S and C-S bonds) and carbon backbones (C-C bonds) [18]. Therefore, we hypothesize that the gut bacteria within mealworms may also play a role in the degradation of vulcanized rubber, and could be a source for isolation of specific microorganisms with the ability to simultaneously break down both sulfide bridges (S-S and C-S bonds) and poly(cis-1, 4-isoprene) backbones within vPR.

In this study, it was the first time to show that a strain *Acinetobacter* sp. BIT-H3, isolated from the gut of mealworm, can utilize the vPR as sole carbon source for growth. To examine whether the vPR degradation was achieved through co-cleavages of sulfide linkages and polymeric backbone within the three-dimensional crosslinking network, the changes in physicochemical properties of vPR after incubation with strain BIT-H3 and the metabolic products released during degradation were characterized. Furthermore, the genes encoding the enzymes responsible for vPR degradation were explored by using the genomic and transcriptional analyses. Last but not least, a biodegradation pathway of vPR for strain BIT-H3 was proposed in terms of the chemical structure changes, degradation products characterizations, and molecular analyses. The findings of this study pave a way for discovering vPR-degrading microorganisms from the gut of insect worm, which would provide opportunities to develop a biodegradation method for vulcanized rubber waste disposal.

2. Materials and methods

2.1. Test rubber materials and media

Vulcanized poly(cis-1,4-isoprene) rubber was prepared by a hot vulcanization process according to GB 6038–2006. Mixture of raw nature rubber (96.5%, w/w), sulfur (2.3%, w/w), zinc oxide (4.0%, w/w), stearic acid (2.0%, w/w), and cyclohexylbenzothiazole sulphenamide (CBS, an accelerator, 1.2%, w/w) was masticated on the mill for 10 min. After then, the mixture was compressed under 30 MPa and cured at 140 °C to form vulcanized rubber. The products were cut into small pieces with size of 5 cm × 1 cm× 0.1 mm (Length × Width × Thickness), and were further extracted by acetone and $CHCl_3$ to remove soluble low-molecular-weight impurities [19]. These extracted pieces were sterilized in 75% ethanol, air-dried in a laminar-flow clean bench and weighted

prior to use.

Mineral salts medium (MSM) was prepared with deionized water (per 1000 mL) containing 0.7 g KH_2PO_4, 0.7 g K_2HPO_4, 1.0 g NH_4NO_3, 0.7 g $MgSO_4 \cdot 7H_2O$, 0.005 g NaCl, 0.002 g $FeSO_4 \cdot 7H_2O$, 0.002 g $ZnSO_4 \cdot 7H_2O$ and 0.001 g $MnSO_4 \cdot H_2O$ and 0.001 g $CuSO_4 \cdot 5H_2O$, then was sterilized by autoclaving at 121 °C for 20 min [14]. The general nutrient media of Luria-Bertani (LB) agar were prepared according to the standard formula.

2.2. Enrichment, isolation, and identification of vulcanized rubber-degrading bacteria

Mealworms (growth age at approximately 3–4 instars) were purchased from Daxing insect-breeding plants in Beijing, China. Approximately 200 of selected mealworms were sterilized via immersion in 75% ethanol for 1 min and then rinsed 2 times with sterile saline water (NaCl, 0.85%, w/v) prior to gut excision. Their guts were sterilely drawn out and pooled into a 50 mL centrifuge tube containing 30 mL of sterile saline water. After being shaken on a vortex mixer for 5 min, the gut tissues were carefully removed with the pipet. The remaining suspension, used as a microbial inoculum, was transferred into a 250 mL Erlenmeyer flask contained 1 g of rubber pieces and 80 mL of MSM. This flask was incubated on a rotary shaker (120 rpm) for 30 days at 30 °C. Then, 30 mL of the enrichment culture was transferred into 80 mL of fresh MSM containing 1 g of rubber pieces, and the cultures were incubated again under the same conditions for 30 days. Then the residual rubber pieces were removed and the cultures were spread on LB agar medium by the standard dilution-plating method. After 5 days of incubation at 30 °C in air atmosphere, individual colonies were randomly picked and streaked repeatedly to obtain pure cultures. The obtained isolates were routinely preserved as both LB medium slants at 4 °C and suspensions with 15% (v/v) glycerol at − 80 °C. Furthermore, these preserved isolates were individually tested in liquid cultures for their ability to grow on vPR.

For taxonomic identification of the obtained isolates, genomic DNA extraction, PCR amplification, and sequencing of the 16 S rRNA gene were carried out according to the previously described method [20,21]. The closest phylogenetic neighbors and the corresponding similarity were determined by aligning the obtained 16 S rRNA sequence against the bacterial type species recorded in the EzBioCloud database [22]. Cell morphology and flagella were observed using scanning electron microscopy (SEM, SU8010, Hitachi) and transmission electron microscopy (TEM, JEM-1400, jeol) after 12 h incubation on LB agar at 30 °C, respectively. The 16 S rRNA sequence of strain BIT-H3 has been deposited in the NCBI GenBank, while the cells of strain BIT-H3 has been deposited at the China Center for Type Culture Collection (CCTCC) in Wuhan, China.

2.3. Biodegradation tests

The isolate was pre-cultured in LB broth at 30 °C for 12 h. Cells were harvested via centrifugation (8000 rpm for 10 min) and washed twice in sterile saline water. The washed cells were re-suspended in sterile MSM to obtain a seed culture of 10^8 cells per mL. For experimental group, 2 mL of seed culture was added into a 100-mL Erlenmeyer flask containing 100 mg of sterile rubber pieces and 18 mL MSM. The flasks with rubber pieces but without inoculum were served as controls, while the flasks with inoculum but without rubber pieces were served as inoculation controls. All cultures were shaken at 120 rpm and 30 °C. Six flasks were prepared for each group in each incubation period of 0, 1, 3, 6, and 10 weeks. Three samples were used for analyzing protein production and weight loss after incubation, while other three samples were used for determine changes in mechanical properties, chemical structures, and the release of degradation products.

2.4. Protein production and weight loss analyses

To determine microbial growth on vPR, total amount of protein from cells in the culture or attached on rubber was determined according to the previously reported method [23,24]. Both culture and residual rubber pieces in each flask were lyophilized and then were re-suspended with 5 mL of distilled water. After addition of 2 mL of 2 M NaOH, the solution was incubated in a boiling water bath for 30 min and then cooled to room temperature. A 0.5-mL portion of each solution was used for protein determination by the method of Bradford. If necessary, the solution was diluted with distilled water. All tests were prepared in triplicate.

To measure weight loss of vPR, the water-insoluble residual rubber pieces and fragmented particles were recovered by filtering the liquid culture through the filter paper (Average pore size: ~3 μm). Subsequently, these recovered residues were washed with warm water (~40 °C) and subsequently dried at 60 °C for 24 h until the weight became constant. With this procedure, the residual weight included the dried weight of residual rubber pieces and fragmented particles. The weight loss of rubber after the incubation was calculated by subtracting the residual weight from the initial weight.

2.5. Physical properties analyses

To examine microbial colonization and surface deterioration morphology, several residual rubber pieces were taken from the culture and immediately soaked with 2.5% glutaraldehyde in 0.1 M phosphate-buffered saline (PBS, pH 7.3) for cell fixation. The pieces were washed two times with 0.1 M PBS (pH 7.3) and post-fixed with 1% osmium tetroxide in 0.1 M PBS (pH 7.3). The post-fixed pieces were dehydrated in ethanol with graded concentrations of 30%, 50%, 70%, 90%, 96%, and 100%, and subsequently undergone the critical point drying with liquid CO_2. The dehydrated samples were sputter-coated with a gold layer and examined using a SEM (Quanta FEG250, FEI).

To determine changes in mechanical properties of the rubber pieces after incubation, the tensile strength of the rubber specimens was characterized on a universal testing machine (AGS-X-1KN, Shimadzu) at a cross-head speed of 100 mm/min according to the standard method GB/T 528–2009. All the results were averaged based on five successful measurements.

2.6. Chemical structures analyses

The cross-linking densities of rubber pieces were measured by using nuclear magnetic resonance cross-linking density spectrometer (VTMR20–010 V-T, Niumag) with an ^{1}H frequency of 21.556 MHz. The spectra were acquired using Carr-Purcell-Meiboom-Gill (CPMG) pulse sequence, while the parameters of $\pi/2$ pulse duration (P90), π pulse duration (P180), Inter-echo time (TE) and Wait time (TW) were set as 2.4 μs, 4.6 μs, 201 μs, and 1000 ms, respectively. All the measurements were carried out at 363.15 K. The cross-linking densities were calculated with the XLD mode.

The sol fractions of rubber pieces after incubation were determined by the swelling test. A 50 mg of sample was immersed in acetone for 48 h, and then transferred into toluene. At the equilibrium swelling time when the rubber can't uptake toluene, the rubber pieces were taken out, weighed, and dried to a constant weight in a vacuum oven at 50 ℃. The sol fractions were calculated according to the following equation, sol fraction = $(W_0 — W_1) / W_0 \times 100\%$, where W_0 is the wet weight of the rubber and W_1 is the dry weight of the rubber.

Surface chemical structures were characterized using attenuated total reflectance-Fourier transform infrared spectroscopy (ATR-FTIR, Nicolet iN10 MX, Thermo Scientific) and X-ray absorption near-edge structure spectroscopy (XANES). Carbon K-edge XANES spectra were measured at beamline B12b of National Synchrotron Radiation Laboratory (NSRL, China), while sulfur K-edge XANES spectra were

measured at beamline 4B7A of Beijing Synchrotron Radiation Facility (BSRF, China).

2.7. Metabolic products analyses

To identify the metabolic products, both culture and residual rubber pieces in each flask were lyophilized into dried solid materials, which were further extracted in Soxhlet apparatus with 500–600 solvent cycles of $CHCl_3$. Then, the $CHCl_3$ was removed from the extracts by evaporation in a rotary evaporator.

On the one hand, the extracts were re-suspended in $CDCl_3$ and further characterized in a 400 MHz nuclear magnetic resonance (NMR) spectrometer (AVANCE III HD, Bruker) with trimethylsilane (TMS) as the internal standard. ^{1}H NMR spectra and ^{13}C NMR spectra were recorded with 32 scans and 1024 scans, respectively. On the other hand, the extracts were re-dissolved in ethyl acetate and then analyzed by a gas chromatography- mass spectrometry (GC-MS) system (7000D GC/TQ, Agilent) with EI mode and ionization energy of 70 eV. The injection volume was 1 μL and the products were separated using a DB5-column (0.1 μm, 0.25 mm × 30 m, Agilen) with helium as carrier gas. The temperature of injection and interface of GC system were set to 250 and 300 °C, respectively. The temperature of column compartment was kept at 50 °C for 3 min, and then raised to 280 °C at 10 °C·min^{-1}, and maintained at the final temperature for 25 min.

The concentration of SO_4^{2-} released into the liquid culture during the rubber degradation was determined by the turbidimetric method with a spectrophotometer according to ASTM D 516–2002 [25].

2.8. PCR and RT-PCR

The genomic DNA was extracted with the MiniBEST Bacteria Genomic DNA Extraction Kit Ver.3.0 (TaKaRa, China), while the whole bacterial RNA was extracted by using TRIzol™ Reagent (Invitrogen, USA). RNA samples were purified using RapidOut DNA Removal Kit (Thermo Scientific, USA) to remove DNA. Reverse transcription reactions were performed to transcript RNA into cDNA by using GoScript™ Reverse Transcription System (Promega, USA). The targeted gene was amplified from DNA or cDNA samples with the designed primer pairs (SI, Table S1) according to the following PCR experimental conditions. The genomic DNA extract or cDNA (1 μL, 300 ng·μL^{-1}), 1 μL of forward and 1 μL of reverse primer, were added to 11 μL of the PCR mixtures (2 × M5 Taq HiFi PCR mix, Mei5 Biotechnology, Beijing). The final volume of PCR mixtures was 20 μL by adding double-distilled H_2O (ddH_2O). PCR was carried out with one denaturation step of 3 min at 95 °C, 35 cycles of 94 °C for 25 s, 55 °C for 0.5 min, 72 °C for 1 min, and a final extension step of 5 min at 72 °C. Amplification products were analyzed by electrophoresis in 1.5% (w/v) agarose gels in 1 × TAE buffer. PCR negative control without DNA or cDNA was also included to test the contamination. PCR controls using RNA samples without reverse transcription step were applied to check for residual DNA in the RNA preparations. Nucleotide sequencing of amplified products were performed by using ABI 3730XL genetic analyzer (Applied Biosystems, CA, USA).

3. Results and discussion

3.1. Screening of vPR-degrading strain BIT-H3

With the gut contents of mealworms as inoculum, an enrichment of microorganisms was obtained by using vPR as the major carbon source for growth. Six bacterial strains belonging to different species were successfully isolated from this enrichment through limiting dilutions on LB agar plates. Subsequently, a primary screening of vPR-degrading microorganisms from these six isolates was carried out, in terms of their growth in MSM medium with vPR as the major carbon source. Only one isolate, named strain BIT-H3, exhibited significant growth after ten

weeks of incubation by measuring the OD_{600} value of liquid culture (SI, Fig. S1). Hence, strain BIT-H3 was selected as potential vPR-degrading microorganism for further investigations.

Strain BIT-H3 was a Gram-negative and facultatively anaerobic bacterium. Colonies of strain BIT-H3 formed on LB agar were circular, smooth, convex, light brown color, and 1.0–1.5 mm in diameter (SI, Fig. S2). SEM and TEM observations showed that cells of strain BIT-H3 were composed of long rod-shaped cells (approx. 0.5–0.7 μm × 4.5–6.2 μm) and coccoid cells (approx. 0.5–0.7 μm × 0.5–1.5 μm) without flagella (Fig. 1a and b). The 16 S rRNA gene sequence of strain BIT-H3 (SI, Table S2) showed a similarity of 95.6–98.1% to the genus *Acinetobacter*, with the highest similarity of 98.18% to the type strain of *Acinetobacter schindleri* CIP 107287. In Fig. 1c, the neighbor-joining (NJ) phylogenetic tree based on 16 S rRNA gene sequences showed that strain BIT-H3 clustered within the species of the genus *Acinetobacter*, and formed an independent phylogenetic line. Based on the morphological characteristics and the results of 16 S rDNA sequencing, it was concluded that the strain BIT-H3 belonged to the genus *Acinetobacter*, for which the name *Acinetobacter* sp. BIT-H3 was proposed. The cells of strain BIT-H3 were preserved at the China Center for Type Culture Collection (CCTCC) with the accession number CCTCC AB 2020194, while the 16 S rRNA gene sequence of strain BIT-H3 was deposited in NCBI under the accession number OQ195075.

3.2. Growth of strain BIT-H3 on vPR

The ability of strain BIT-H3 to degrade and grow on vPR was substantiated by analyzing the weight loss of vPR pieces in the presence or absence of strain BIT-H3 and the protein production of strain BIT-H3 grown with or without vPR pieces as sole carbon source. To ensure that strain *Acinetobacter* sp. BIT-H3 is really able to degrade the vulcanized rubber but not the low-molecular-weight impurities (such as low molecular-weight monomers, oligomers, and organic chemical additives) as sole carbon source, the used vPR pieces were extracted by acetone and $CHCl_3$ to remove soluble low-molecular-weight impurities before biodegradation experiment [19].

Fig. 2a presented the evolution of weight loss for vPR pieces inoculated with or without strain BIT-H3. During the incubation period, the weight loss of inoculated vPR pieces increased consistently, whereas the weight loss of un-inoculated control was negligible. After ten weeks, the maximum weight loss of vPR pieces inoculated with strain BIT-H3 reached up to 12 ± 1.1%, which was similar to the weight loss of vulcanized latex glove caused by the three previously reported Gram-negative rubber-degrading bacteria strains, *Xanthomonas* sp., *Pseudomonas citronellolis* and *Acinetobacter calcoaceticus* [24]. This result reveals that the weight loss of inoculated rubber pieces could be attributed to biological activity of strain BIT-H3 other than abiotic process.

Fig. 2b showed the time course of protein production by strain BIT-H3 incubated with or without vPR as the major carbon source. When strain BIT-H3 was incubated in MSM medium with vPR, the protein concentration of culture increased up to 406 ± 19 μg/mL after ten weeks of incubation. By comparison, the protein concentration of the control culture, in which strain BIT-H3 was incubated without vPR and other organic nutrients, kept constant in a low level of 50 μg/mL over the incubation time. Based on the results of protein production and weight loss, the protein yield of strain BIT-H3 incubated with vPR pieces as sole carbon source could be estimated as 0.67 ± 0.01 g protein per g rubber pieces. This reveals that strain BIT-H3 is able to use vPR as the source of carbon for protein synthesis.

Moreover, SEM was used to visually examine the ability of strain BIT-H3 to grow on and degrade vPR pieces. As showed in Fig. 2c, the surface of an un-inoculated control remained smooth and without any defects. In contrast, on the surface of samples inoculated with strain BIT-H3, the cells of strain BIT-H3 were able to penetrate into the vPR pieces and produce several colony craters (about 10–20 μm in diameter) since the beginning of first week (Fig. 2d). Within the second week, the colony
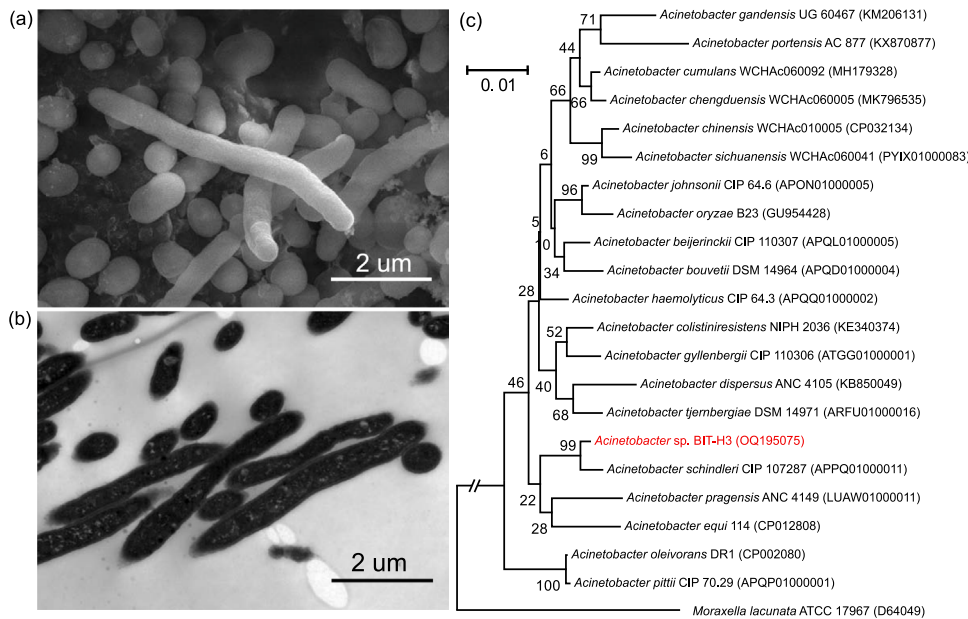
Fig. 1. Micrographs and taxonomic identification of strain BIT-H3. (a) Scanning electron micrograph of strain BIT-H3; (b) Transmission electron micrograph of strain BIT-H3; (c) Neighbor-joining phylogenetic tree based on based on 16S rRNA gene sequences of strain BIT-H3 and its closely related type species. Bootstrap values based on 1000 replicates are expressed as percentages. The 16S rRNA gene sequence of *Moraxella Iacunata* ATCC 17967^T was used as an outgroup. Bar, 0.01 substitutions per nucleotide position.
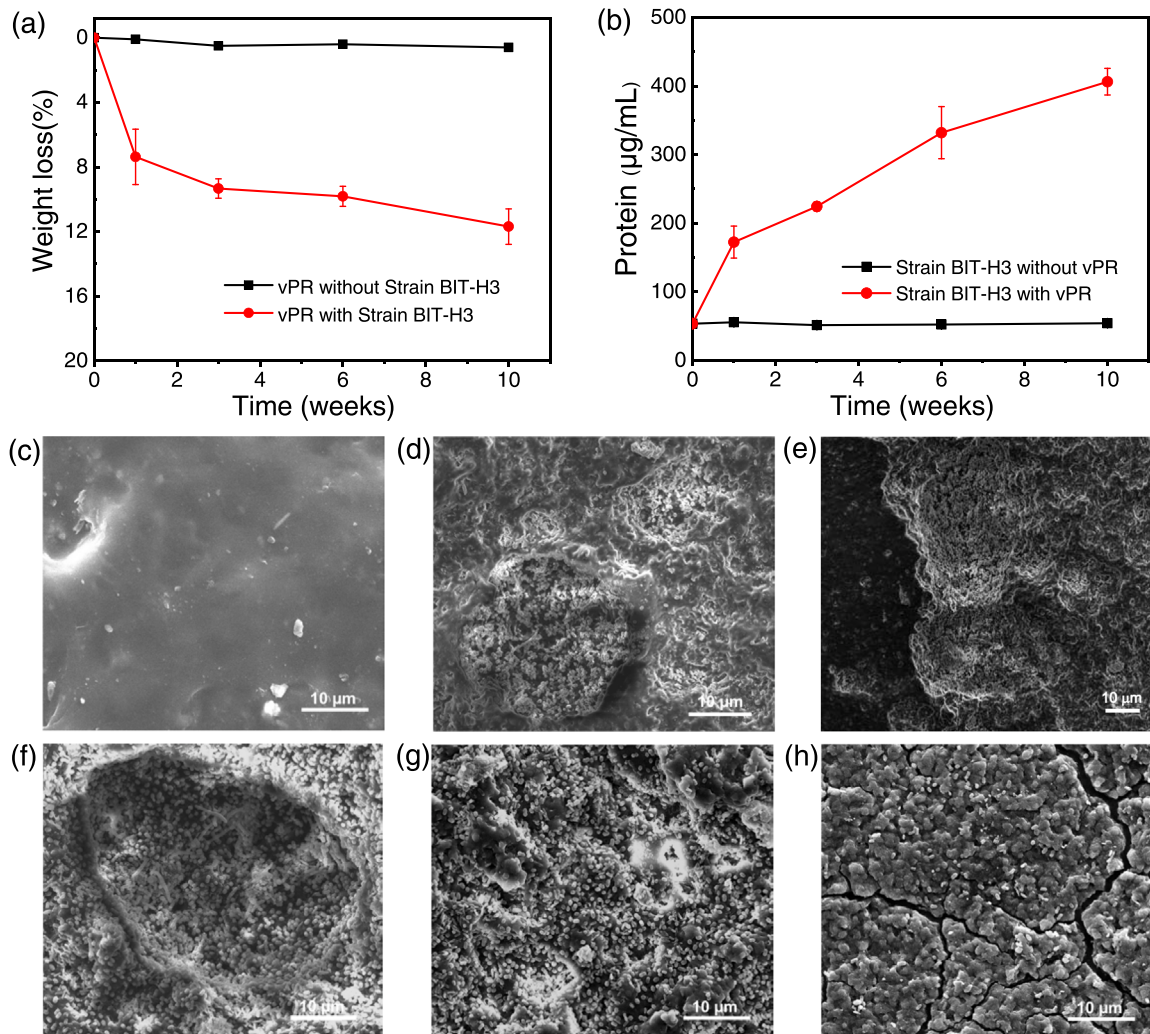

Fig. 2. Growth of strain BIT-H3 on vPR. (a) Weight loss of vPR during ten weeks of incubation in the presence or absence of strain BIT-H3 (mean value $\pm$ SD, $n = 3$); (b) Protein concentration of strain BIT-H3 culture incubated with or without vPR (mean value $\pm$ SD, $n = 3$); (c) Scanning electron micrographs of surface topography on the sterile controls, and vPR pieces inoculated with strain BIT-H3 after one week (d), two week (e), three week (f), six weeks (g), and ten weeks (h).

craters became larger and deep (Fig. 2e). After three weeks, strain BIT-H3 could form a compact biofilm across the surface and extend the area of colony crater up to about 45 μm in diameter (Fig. 2f). At the end of six weeks, the edges of colony crater almost disappeared and several convex structures formed on the surface of inoculated samples (Fig. 2g). After ten weeks' incubation, the convex structures have deteriorated into a large amount of small granular pimples and several obvious cracks appeared (Fig. 2h). These observations unequivocally demonstrate that strain BIT-H3 was not only able to adhesively grow on the surface of vPR pieces, but also bring about significant disintegration to this material.

3.3. Decrosslink of vPR by strain BIT-H3

The ability of strain BIT-H3 to degrade vPR was further verified by investigating the changes in mechanical property and chemical structure of the residual vPR recovered after inoculation with or without strain BIT-H3.

First, the tensile strength of vPR pieces inoculated with or without strain BIT-H3 was tested to determine the changes in mechanical property. As can be seen in Fig. 3a, the tensile strength of samples inoculated with strain BIT-H3 dramatically decreased from 78.2 ± 4.2 MPa to 36.6 ± 1.2 MPa, and the maximum loss rate of tensile strength came up to about 53.2%. In contrast, the tensile strength of un-inoculated controls was almost unchanged over the ten weeks of

incubation time. This supports the observation of vPR degradation by strain BIT-H3 through weight loss measurements and SEM investigations.

Next, the detail changes in chemical structure were characterized underlying the degradation of vPR by strain BIT-H3. Due to the insolubility of vPR in organic solvent caused by its stable three-dimensional crosslinking network structure, the changes in crosslink density, instead of molecular weight, was characterized as a key indicator for scission of three-dimensional crosslinking network within vPR [26–28]. As seen in Fig. 3b, the crosslink density of vPR inoculated with strain BIT-H3 decreased from $2.05 \pm 0.51 \times 10^{-4}$ mol/cm^3 to $1.47 \pm 0.11 \times 10^{-4}$ mol/cm^3 over the ten weeks' incubation period. The highest decrement of crosslink density reached up to about 29.3%. By comparison, the crosslink density of un-inoculated control was almost unchanged. This finding reveals that the three-dimensional crosslinking network structure of vPR was broken by strain BIT-H3.

Furthermore, to determine which part of the crosslinking network structure, polymeric chains or sulfide bridges, has been broken by strain BIT-H3, a Horikx analysis (SI, M1) was performed according to the theoretical relationship between sol fraction and crosslink density during the degradation of vulcanized rubber [26]. As shown in Fig. 3c, the dotted curve was assigned to polymeric backbone scission while the solid curve was denoted as sulfide bridges scission. The experimental samples inoculated with strain BIT-H3 from different time points located
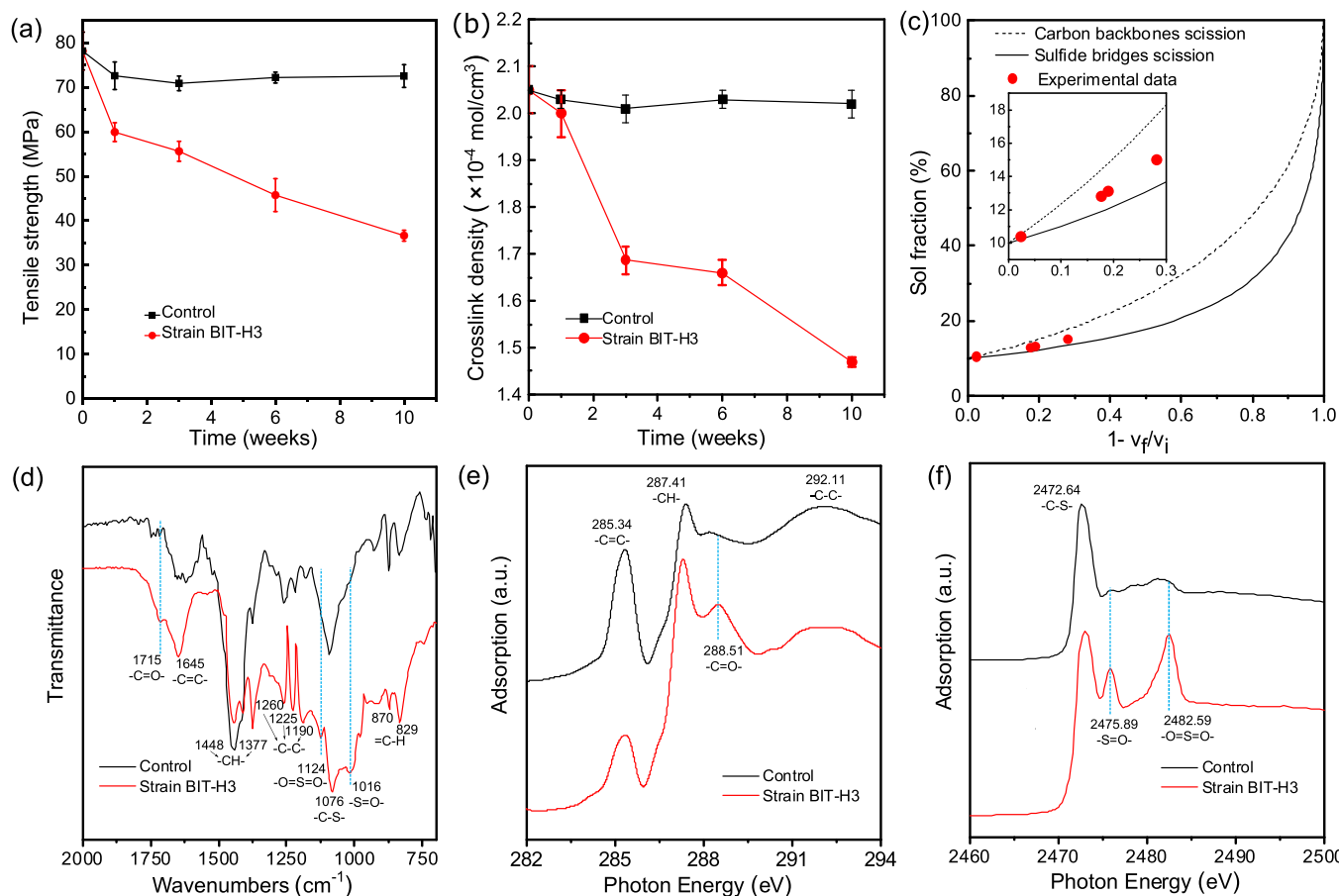

Fig. 3. Changes in mechanical property and chemical structure of vPR degraded by strain BIT-H3. (a) The changes in tensile strength of vPR in the presence or absence of strain BIT-H3 during ten-week period (mean value ± SD, $n = 3$); (b) The changes in crosslinking density of vPR in the presence or absence of strain BIT-H3 during ten-week period (mean value ± SD, $n = 3$); (c) The sol fraction against relative crosslink density of vPR degraded by strain BIT-H3 during ten-week period. v_i and v_f are the crosslink densities of vPR before and after degradation. The solid curve or the dotted curve is plotted according to the Horikx equations (SI, M1), and corresponds to the situation in which either only crosslinks or polymeric backbone were broken, respectively. The area between the solid curve and the dotted curve corresponds to the situation in which both crosslinks and polymeric backbone were broken; (d) FTIR spectra of sterile control versus vPR degraded by strain BIT-H3 after ten weeks; (e) The carbon *K*-edge XANES spectra of sterile control versus vPR degraded by strain BIT-H3 after ten weeks; (f) The sulfur *K*-edge XANES spectra of sterile control versus vPR degraded by strain BIT-H3 after ten weeks.

in the interspace between two curves, but not close to either of two curves. This observation indicates that the scissions of polymeric backbone and sulfide bridges occurred simultaneously during the degradation process [26–28].

The ATR-FTIR spectroscopy were further used to confirm the co-scissions of polymeric backbone and sulfide bridges during the degradation process. Prior to the analyses, the microbial biofilm colonized on the surfaces of samples were clearly removed [29]. Fig. 3d illustrated the ATR-FTIR spectrum of vPR sample inoculated with strain BIT-H3 versus that of un-inoculated control after ten weeks' incubation period. Both of two spectra shared the general peaks corresponding to the standard spectrum of poly(*cis*-isoprene) rubber, such as the peaks of –C═C– bonds at 1645 cm⁻¹, saturated –CH₂– bending vibrations at 1448 cm⁻¹ and 1337 cm⁻¹, –C–C– bonds at 1260 cm⁻¹, 1225 cm⁻¹, and 1190 cm⁻¹, ═CH– bending vibrations at 870 cm⁻¹ and 829 cm⁻¹ [28,29]. Additionally, the peaks of –C–S– bonds at 1076 cm⁻¹, a sign of cross-linked sulfide bridges, were also observed in all spectra [27]. However, the intensities of –C═C– peak at 1645 cm⁻¹ and –C–S– peak at 1076 cm⁻¹ were obviously reduced in the spectrum of inoculated vPR sample by comparison with that of un-inoculated control. Meanwhile, in the spectrum of inoculated vPR sample, three new peaks appeared at 1715 cm⁻¹, 1124 cm⁻¹, and 1016 cm⁻¹ could be assigned to carbonyl bonds –C═O– [27–29], sulfone bonds –O═S═O– [28], and sulfoxide bonds –S═O– [27], respectively. These results reveal that strain BIT-H3 could oxidatively cleave the –C═C– bonds of poly(*cis*-isoprene) backbone and the –C–S– bond of cross-linked sulfide bridges to produce new carbonyl bonds –C═O–, sulfone bonds –O═S═O–, and sulfoxide bonds –S═O–. Notably, the amide bands assigned for protein at 1652 cm⁻¹ and 1545 cm⁻¹, and the polysaccharide bands in the region from 900 to 1200 cm⁻¹ were not observed in the FTIR spectrum of inoculated vPR sample (Fig. 3d), indicating that the biofilm was clearly removed from the surface and the contamination of specific marker bands from microbial biomass could be excluded [29].

XANES analysis is a precise technique for studying the local atom information in solid materials and has been used to characterize the oxidative degradation of vulcanized nature rubber and waste tire rubber [30,31]. Fig. 3e illustrated the carbon *K*-edge XANES spectra of vPR sample inoculated with strain BIT-H3 and un-inoculated control. Both of two spectra have the peaks at 285.34 eV, 287.31 eV, and 292.11 eV, which were assigned to the 1π* –C═C–, σ * –CH–, and σ * –C–C– resonance of poly(*cis*-isoprene) backbone, respectively [32]. However, the adsorption intensity of 1π* –C═C– peak at 285.34 eV in the spectrum of inoculated vPR sample showed a significant reduction than that of un-inoculated control, while a newly peak of 1π* –C═O– at 288.51 eV appeared in the spectrum of inoculated vPR sample. These results could be considered as a suggestive marker for oxidative cleavage of –C═C– bonds in poly(*cis*-isoprene) backbone [32]. Meanwhile, Fig. 3f exhibited the sulfur *K*-edge XANES spectra of vPR sample inoculated with strain BIT-H3 and un-inoculated control after ten weeks' incubation. Both of two spectra showed a sharp absorption peak at 2472.64 eV, corresponding to the σ * –S–C– resonance or σ * –S–S– resonance of cross-linked sulfide bridges [30,31]. But, the adsorption intensity of σ * –S–C– (σ * –S–S–) peak at 2472.64 eV in the spectrum of inoculated vPR sample showed a significant reduction in comparison with that of un-incubated control. Additionally, two newly peak of σ * –S═O– at 2475.89 eV and σ * –O═S═O– at 2482.59 eV appeared in the spectrum of inoculated vPR sample, which could be assigned to the partially oxidized sulfur species sulfoxide and sulfone [30,31]. Taken together, all results of carbon and sulfur *K*-edge XANES analyses agree with the data of ATR-FTIR and further support the oxidative cleavage of the –C═C– bonds of poly(*cis*-isoprene) backbone and the sulfide bridges by strain BIT-H3.

3.4. Products released from vPR decrosslink by strain BIT-H3

To further provide evidence for the ability of strain BIT-H3 to cleave

the –C═C– bonds of poly(*cis*-isoprene) backbone and the cross-linked sulfide bridges within vPR, the released organic and inorganic products was analyzed during the incubation.

Sulfate has been reported as the final metabolic product of the cleaved cross-linked sulfide bridges form vulcanized rubber [25,30,33]. Fig. 4a showed the time-courses of sulfate concentrations in the culture containing vPR pieces in the presence or absence of strain BIT-H3. Sulfate concentrations of inoculated culture increased substantially during the ten weeks of incubation. The highest sulfate concentration reached up to 513.8 ± 11.1 mg/L after ten weeks of incubation. However, sulfate concentrations of un-inoculated control remained constant along the incubation time. This result strongly demonstrates that strain BIT-H3 is able to cleave the sulfide bridges of vPR and then convert the cleaved sulfide bridges into sulfate as the final products.

The organic degradation products were extracted from the culture after ten weeks of incubation period and subsequently analyzed by NMR spectroscopy [34–37]. To avoid interference from the medium and microbial metabolites, the products extracted from un-inoculated controls and the inoculated glucose-grown culture were also examined with the same method. As seen in Fig. 4b, in comparison with the ¹H NMR spectrum of culture from un-inoculated controls or inoculated glucose-grown culture, the ¹H NMR spectrum of inoculated vPR culture showed the peaks at 5.15 ppm, 2.07 ppm and 1.71 ppm, which represented olefinic protons (═CH–), methylene protons (–CH₂–) and methyl protons (–CH₃) of the structure of poly(cis-1,4-isoprene), respectively (marked by numbers 1, 2 and 3 in Fig. 4d) [34–37]. Two small signals at 9.69 ppm and 2.23 ppm could be assigned to proton of terminal aldehyde group (–CHO) and the protons of the methyl ketone (CH₃–C (═O)–), respectively (marked by numbers 4 and 5 in Fig. 4d) [34,36]. Furthermore, the ¹³C NMR spectrum (Fig. 4c) of inoculated vPR culture exhibited five strong peaks at 134.2 ppm, 124.1 ppm, 31.2 ppm, 25.4 ppm, and 22.4 ppm, which can be associated with the repeated structure of the poly(cis-1,4-isoprene) backbone (marked by alphabets A, B, C, D and E in Fig. 4d) [34,36]. The signals at 175.3 ppm and 175.1 ppm were corresponding to the carbonyl carbon of the terminal aldehyde group and the methyl ketone, respectively (marked by alphabets F and G in Fig. 4d) [34,36]. Based on the combined results of ¹H NMR and ¹³C NMR, the chemical structure of the degradation products could be identified as a oligo(cis-1,4 isoprene) with terminal aldehyde and keto groups (Fig. 4d), which was consistent with the previous reports about the degradation products of poly(cis-1,4-isoprene) using bacterial cultures and enzymes [34–37]. Nevertheless, the intensities of peaks corresponding to the terminal aldehyde group and the methyl ketone were significantly lower than that of the signals from the isoprene repetitive units, indicating that the major degradation products detected by NMR may be long-chain oligomers with a varying number of repetitive units (–CH₂–C(CH₃)═CH–CH₂–) [37].

Furthermore, the low-molecular weight organic degradation products were analyzed by GC-MS [38,39]. In comparison with the GC-MS chromatograms of extraction from un-inoculated controls or inoculated glucose-grown culture, the GC-MS chromatogram of extraction from inoculated vPR showed six unique peaks at the retention time of 12.35 min, 12.88 min, 13.25 min, 18.57 min, 21.22 min, and 22.63 min, respectively (SI, Fig. S3a). Furthermore, the components at the six retention times in GC-MS chromatogram were analyzed by using mass spectrometry (SI, Figs. S3b and S4). The product corresponding to the retention time of 12.35 min, 12.88 min, 13.25 min, 18.57 min, 21.22 min, and 22.63 min was identified as Benzaldehyde, 2, 5-dimethyl- (CAS# 5779–94–2), Benzaldehyde, 4-propyl- (CAS# 28785–06–0), Cyclooctasiloxane, hexadecamethyl- (CAS# 556–68–3), 9,12,15-Octadecatrienoicacid, 2,3-dihydroxypropyl ester, (*Z,Z,Z*)- (CAS# 18465–99–1), Tetracosa-2,6,14,18,22-pentaene-10,11-diol, 2,6, 10,15,19,23-hexamethyl- (CAS# 166048–00–6), (2E,6E,10E,14E)– 3, 7,11,15,19-Pentamethyl-2,6,10,14,18-icosapentaenoic acid (CAS# 64284–92–0), respectively. Among them, the latter three products may represent the low-molecular weight degradation products (< 600 Da)
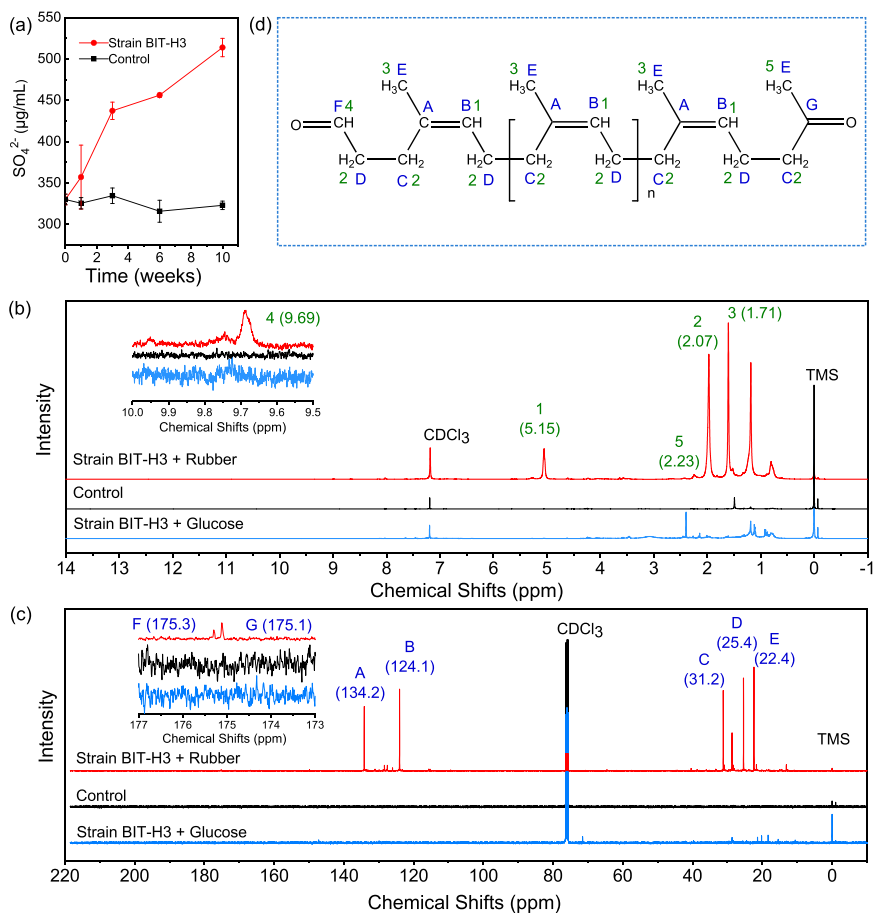
Fig. 4. Degradation products released during vPR degradation by strain BIT-H3. (a) Sulfate concentrations in the culture containing vPR pieces in the presence or absence of strain BIT-H3; (b) ^{1}H NMR spectra and (c) ^{13}C NMR spectra of degradation products extracted from the vPR-grown culture inoculated with strain BIT-H3, un-inoculated controls, and the inoculated glucose-grown culture. (d) The degradation products structure of the oligo(cis-1,4 isoprene) with terminal aldehyde and keto groups according to the characterization of ^{1}H NMR and ^{13}C NMR spectra.

released during vPR degradation because they have the same repetitive unit (—CH$_2$—C(CH$_3$)=CH—CH$_2$—) with the poly(cis-1,4-isoprene) (SI, Fig. S4).

3.5. Identification and transcription of genes encoding desulfurases and rubber oxygenases

The microbial desulfurization pathway, known as the 4 S pathway, has been described to be catalyzed by three enzymes of DszA, DszB, and DszC encoded by a *dsz* operon [4,7]. Meanwhile, three rubber oxygenases of Lcp, RoxA, and RoxB together with laccase and peroxidase have been reported to be able to cleave the double bonds of poly(cis-1,4-isoprene) chain [10,40,41]. To identify orthologues of the reported genes encoding enzymes related to the oxidative cleavage of sulfur bridges and polymeric backbone within vPR, the sequencing and functional analysis of strain BIT-H3 genome was carried out. A *dsz*-like operon comprised of three open reading frames (ORF) was found in the genome of strain BIT-H3 (SI, Table S3). In this *dsz*-like operon, the first open reading frame (ORF), *dszA*, had 31.1% amino acid (aa) identity to *DszA* of *Rhodococcus erythropolis* XP, while the second and third ORF, named *dszC1* and *dszC2*, had 26.3% and 22.3% aa identity to *DszC* of *Rhodococcus erythropolis* XP, respectively [7]. The aa identity between *dszC1* and *dszC2* was 38.8%. The *dsz*-like operon lacked the gene *DszB* encoding DBT-sulfonate desulfinase and no other homologs of the *DszB* were found in the genome of strain BIT-H3. In addition, one gene encoding laccase-like enzyme (Laccase 2147) and other gene encoding peroxidase-like enzyme (Peroxidase 1232) were recovered from the genome of strain BIT-H3 (SI, Table S3), despite no homologs of the three well characterized rubber oxygenases, such as Lcp, RoxA, and RoxB, were found in the genome. Both the Laccase 2147 and Peroxidase 1232 carried signal peptides for extracellular localization via the Sec pathway.

Moreover, transcriptional expression of the five functional genes of *dszA*, *dszC1*, *dszC2*, Laccase2147, and Peroxidase1232 was examined to assess the involvement of these genes in the degradation of vPR by strain BIT-H3 [42]. Qualitative reverse transcription PCR (RT-PCR) was performed with DNA-free RNAs extracted from the cells of strain BIT-H3 grown on glucose or vPR. The specific primers for the above five functional genes and the control of 16 S rRNA gene were used to estimate the transcriptional level (SI, Table S1). As seen in Fig. 5a, the strong bands for the PCR products of *dszA* (1425 bp), *dszC1* (1224 bp), *dszC2* (1203 bp), Laccase 2147 (1293 bp), and Peroxidase 1232 (1203 bp) yielded in the cDNA sample from the cells grown on vPR but not in that from the cells grown on glucose. In contrast, the PCR products of housekeeping gene of 16 S rRNA appeared in both of cDNA samples from the cells grown on glucose or vPR. This results clearly reveal that the five functional genes of *dszA*, *dszC1*, *dszC2*, Laccase2147, and Peroxidase1232 were transcribed in cells incubated in the presence of vPR other than glucose. The absence of PCR products in the control RNA samples without the RT reaction step indicates that the RT-PCR product (PCR product of cDNA) was not derived from contaminating DNA (Fig. 5a). The significant transcription of the five functional genes of *dszA*, *dszC1*, *dszC2*, Laccase2147, and Peroxidase1232 in the presence of vPR other than glucose suggests the involvement of these genes in the degradation of vPR by strain BIT-H3.

3.6. Proposed mechanism for vPR degradation by strain BIT-H3

Based on the above results of chemical structure changes, metabolic products analysis, and genomic and transcriptional analyses of function genes, a possible mechanism for the degradation of vPR by strain BIT-H3 was schematically exhibited in Fig. 5b. In brief, the degradation process of vPR can be divided into three steps: devulcanization,
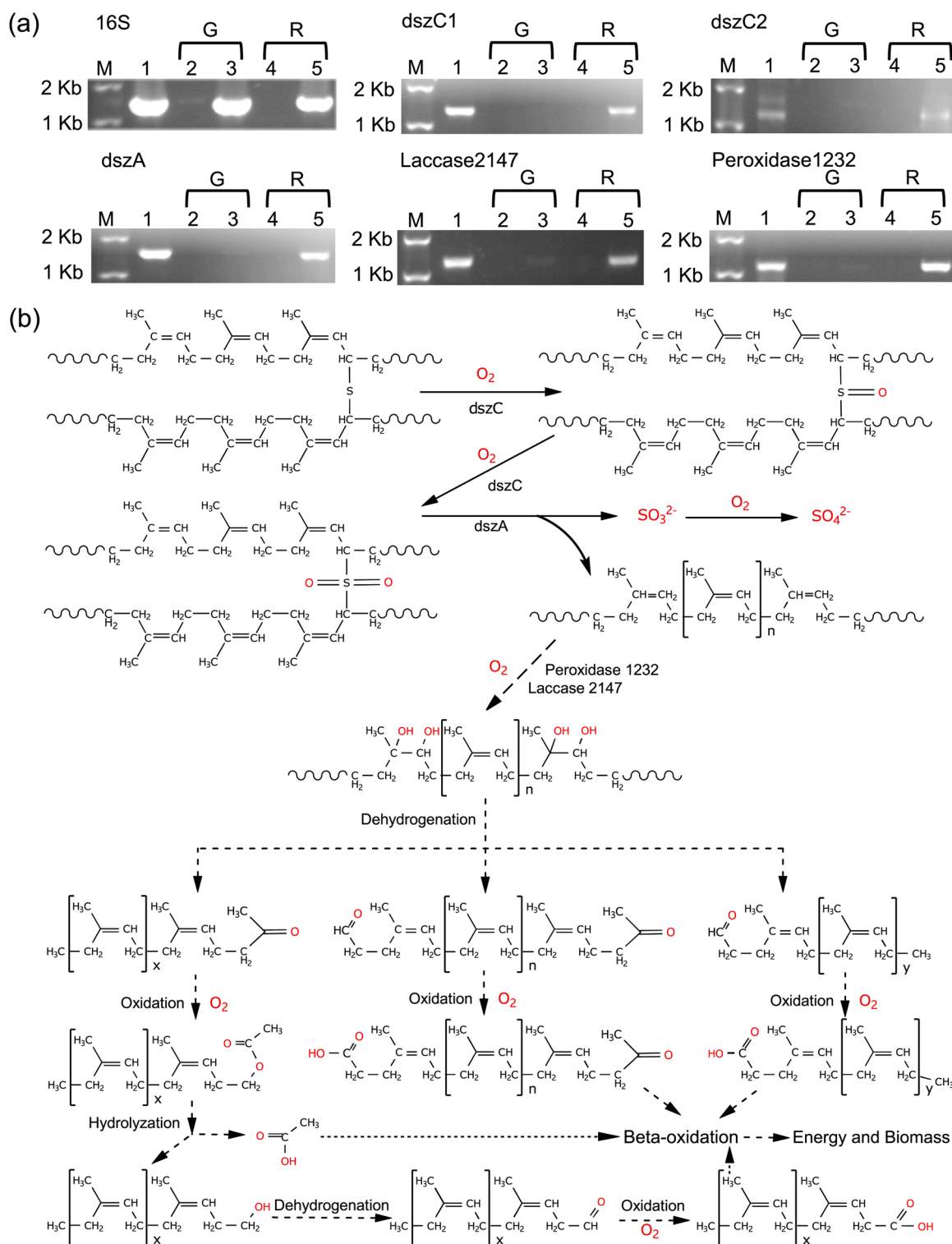
Fig. 5. Expression of degradative enzymes and mechanism for vPR degradation by strain BIT-H3. (a) Transcription level of three genes encoding desulfurases and two genes encoding rubber oxygenases in strain BIT-H3. RT-PCR amplification of mRNA for five genes from the strain BIT-H3 incubated with vPR (R) or glucose (G) as the carbon source. Lane 1 represents the control PCR product of gene directly amplified from genomic DNA of strain BIT-H3. Lane 2 and lane 4 represent the PCR products amplified from RNA samples treated with DNase in the absence of RT, in which the absence of PCR products indicates that there is no DNA contaminant in the RNA samples. Lane 3 and lane 5 represent the PCR products amplified from RNA samples treated with DNase in the presence of RT. (b) Proposed pathway of vPR degradation by strain BIT-H3 based on the results of chemical structure changes, degradation products analyses, genome and transcription analyses.

depolymerization, and assimilation [5,6].

In the devulcanization step, the crosslink bonds of sulfide bridges are broken down via the "4S" pathway by the action of a series of enzymes encoded by a *dsz* operon [5,6]. At the beginning, dszC1 or dszC2

catalyze the oxidation of sulfide bridges into sulfoxide bridges and then to sulfone bridges. Subsequently, dszA catalyze the cleavage of sulfone bridges, resulting in the release of sulfite (Spontaneously oxidized into sulfate as final products) and the formation of linear poly(*cis*-isoprene)

macromolecules.

In the next step of depolymerization, the long chains of poly(*cis*-isoprene) are cleaved into small fragments. Initially, the oxidation of C═C bonds in the long poly(*cis*-isoprene) chains is catalyzed by Laccase 2147 or Peroxidase 1232. Next, the oxidized long poly(*cis*-isoprene) chains are further cleaved via dehydrogenation, leading to the reduction of molecular weight and the production of *cis*-1,4-isoprene oligomers with terminal keto and aldehyde groups. This oxidative cleavage process may repeat several times, generating the small oligomers with sufficiently low molecular weight that could be transported across the cell membrane into the cells of strain BIT-H3.

In the assimilation step, the aldehyde groups of small oligomers generated by the depolymerization process could be further oxidized by aldehyde dehydrogenase into carboxylic acids. Concurrently, the keto groups of small oligomers generated by the depolymerization process could be further oxidized into ester groups, which could be further hydrolyzed into the carboxylic acids and alcohols. The alcohols are further oxidized by alcohol and aldehyde dehydrogenases into carboxylic acids. According to the previous reports [6,23,24], the small oligomers with the terminal carboxyl groups could be degraded through the β-oxidation to generate Acetyl-CoA and propionyl-CoA, which can ultimately enter into the tricarboxylic acid cycle (TCA cycle) and provide energy and carbon source for growth of strain BIT-H3.

4. Conclusion

In this work, for the first time, a bacterium *Acinetobacter* sp. BIT-H3 capable of growing on vulcanized poly(*cis*-isoprene) rubber as sole carbon source is isolated from the gut of mealworm. This gut bacterium is demonstrated to be able to degrade vulcanized poly(*cis*-isoprene) rubber by simultaneously cleaving both sulfide bridges and C═C bonds of poly(*cis*-isoprene) backbone within the cross-linked network of vulcanized poly(*cis*-isoprene) rubber. Using the genomic and transcriptional analyses, three genes of *dszA*, *dszC1*, and *dszC2* encoding desulfurases and two genes of *Laccase2147* and *Peroxidase1232* encoding rubber oxygenases are found to be involved in the degradation of vulcanized poly(*cis*-isoprene) rubber by strain BIT-H3. Our findings indicate that the gut bacterium BIT-H3 from plastic-eating mealworm can overcome the obstacles of three-dimensional crosslinking network structure and effectively degrade the vulcanized rubber. This could have implications for further application of this strain in the disposal of vulcanized rubber waste, upcycling the products released during vPR degradation, and modifying the interface compatibility of waste rubber particles for manufacturing composite.

Besides vulcanized poly(*cis*-isoprene) rubber, there are many another types of vulcanized rubber products with different composition, such as styrene butadiene rubber, butadiene rubber, and chloroprene rubber. As this study has demonstrated that the gut bacteria of plastic-eating mealworm is a promising source for isolation of vulcanized poly(*cis*-isoprene) rubber-degrading strain, further work is need to exploring more diverse vulcanized rubber-degrading microorganisms from the gut of plastic-eating insect larvae.

CRediT authorship contribution statement

Yu Yang: Conceptualization, Methodology, Data analysis, Validation, Writing – original draft, Writing – review & editing, Funding acquisition, Supervision. **Xiaotao Cheng:** Methodology, Writing – original draft. **Mengli Xia:** Data analysis, Methodology.

Declaration of Competing Interest

The authors declare that they have no known competing financial interests or personal relationships that could have appeared to influence the work reported in this paper.

Data availability

Data will be made available on request.

Appendix A. Supplementary material

Primer sequences used in RT-PCR (Table S1). Full sequence of 16 S rRNA gene form strain BIT-H3 (Table S2). Sequences of genes encoding rubber desulfurases and oxygenases (Table S3). Growth curves of six bacterial strains belonging to different species isolated from the enrichment of gut microbiota with vPR as the major carbon source in MSM (Fig. S1). Photograph of strain BIT-H3 colonies growing on LB agar plate (Fig. S2). GC-MS analysis of degradation products released during vPR degradation by strain BIT-H3 (Fig. S3). Mass spectrometry analyses of the components at the six unique retention times in GC-MS chromatograms (Fig. S4). Supplementary data associated with this article can be found in the online version at doi:10.1016/j.jhazmat.2023.130 940.

References

[1] Chittella, H., Yoon, L.W., Ramarad, S., Lai, Z.W., 2021. Rubber waste management: a review on methods, mechanism, and prospects. Polym Degrad Stab 194, 109761.

[2] Singh, E., Kumar, A., Mishra, R., Kumar, S., 2022. Solid waste management during COVID-19 pandemic: recovery techniques and responses. Chemosphere 288, 132451.

[3] Wang, Z., An, C., Lee, K., Chen, X., Zhang, B., Yin, J., et al., 2022. Physicochemical change and microparticle release from disposable gloves in the aqueous environment impacted by accelerated weathering. Sci Total Environ 832, 154986.

[4] Jędruchniewicz, K., Ok, Y.S., Oleszczuk, P., 2021. COVID-19 discarded disposable gloves as a source and a vector of pollutants in the environment. J Hazard Mater 417, 125938.

[5] Stevenson, K., Stallwood, B., Hart, A.G., 2008. Tire rubber recycling and bioremediation: a review. Bioremediat J 12 (1), 1–11.

[6] Andler, R., 2020. Bacterial and enzymatic degradation of poly(cis-1,4-isoprene) rubber: Novel biotechnological applications. Biotechnol Adv 44, 107606.

[7] Oldfield, C., Pogrebinsky, O., Simmonds, J., Olson, E.S., Kulpa, C.F., 1997. Elucidation of the metabolic pathway for dibenzothiophene desulphurization by *Rhodococcus* sp. strain IGTS8 (ATCC 53968). Microbiology 143, 2961–2973.

[8] Jendrossek, D., Birke, J., 2019. Rubber oxygenases. Appl Microbiol Biotechnol 103 (1), 125–142.

[9] Nayanashree, G., Thippeswamy, B., 2015. Biodegradation of natural rubber by laccase and manganese peroxidase enzyme of *Bacillus subtilis*. Environ Process 2 (4), 761–772.

[10] Andler, R., D'Afonseca, V., Pino, J., Valdés, C., Salazar-Viedma, M., 2021. Assessing the biodegradation of vulcanised rubber particles by fungi using genetic, molecular and surface analysis. Front Bioeng Biotechnol 9, 761510.

[11] Yang, Y., Yang, J., Wu, W.-M., Zhao, J., Song, Y., Gao, L., et al., 2015. Biodegradation and mineralization of polystyrene by plastic-eating mealworms: part 1. Chemical and physical characterization and isotopic tests. Environ Sci Technol 49, 12080–12086.

[12] Yang, Y., Yang, J., Wu, W.-M., Zhao, J., Song, Y., Gao, L., et al., 2015. Biodegradation and mineralization of polystyrene by plastic-eating mealworms: Part 2. Role of gut microorganisms. Environ Sci Technol 49, 12080–12086.

[13] Yang, Y., Hu, L., Li, X., Wang, J., Jin, G., 2023. Nitrogen fixation and diazotrophic community in plastic-eating mealworms *Tenebrio molitor* L. Microb Ecol 85, 264–276.

[14] Yang, J., Yang, Y., Wu, W.-M., Zhao, J., Jiang, L., 2014. Evidence of polyethylene biodegradation by bacterial strains from the guts of plastic-eating waxworms. Environ Sci Technol 48, 13776–13784.

[15] Ru, J., Huo, Y., Yang, Y., 2020. Microbial degradation and valorization of plastic wastes. Front Microbiol 11, 442.

[16] Kim, H.R., Lee, H.M., Yu, H.C., Jeon, E., Lee, S., Li, J., et al., 2020. Biodegradation of polystyrene by *pseudomonas* sp. isolated from the gut of superworms (Larvae of *Zophobas atratus*). Environ Sci Technol 54 (11), 6987–6996.

[17] Brandon, A.M., Garcia, A.M., Khlystov, N.A., Wu, W.M., Criddle, C.S., 2021. Enhanced bioavailability and microbial biodegradation of polystyrene in an enrichment derived from the gut microbiome of *Tenebrio molitor* (Mealworm Larvae). Environ Sci Technol 55 (3), 2027–2036.

[18] Aboelkheir, M.G., Visconte, L.Y., Oliveira, G.E., Toledo Filho, R.D., Souza Jr., F.G., 2019. The biodegradative effect of *Tenebrio molitor* Linnaeus larvae on vulcanized SBR and tire crumb. Sci Total Environ 649, 1075–1082.

[19] Heisey, R.M., Papadatos, S., 1995. Isolation of microorganisms able to metabolize purified natural rubber. Appl Environ Microbiol 61 (8), 3092–3097.

[20] Xia, M., Wang, J., Huo, Y.X., Yang, Y., 2020. *Mixta tenebrionis* sp. nov., isolated from the gut of the plastic-eating mealworm *Tenebrio molitor* L. Int J Syst Evol Microbiol 70 (2), 790–796.

[21] Hu, L., Yang, Y., 2022. *Tenebrionibacter intestinalis* gen. nov., sp. nov., a member of a novel genus of the family *Enterobacteriaceae*, isolated from the gut of the plastic-eating mealworm *Tenebrio molitor* L. Int J Syst Evol Microbiol 72 (2), 5246.

[22] Yoon, S.H., Ha, S.M., Kwon, S., Lim, J., Kim, Y., Seo, H., et al., 2017. Introducing EzBioCloud: a taxonomically United database of 16S rRNA gene sequences and whole-genome assemblies. Int J Syst Evol Microbiol 67, 1613–1617.

[23] Bode, H.B., Zeeck, A., Plückhahn, K., Jendrossek, D., 2000. Physiological and chemical investigations into microbial degradation of synthetic Poly(cis-1,4-isoprene). Appl Environ Microbiol 66 (9), 3680–3685.

[24] Bode, H.B., Kerkhoff, K., Jendrossek, D., 2001. Bacterial degradation of natural and synthetic rubber. Biomacromolecules 2 (1), 295–303.

[25] Jiang, G., Zhao, S., Luo, J., Wang, Y., Yu, W., Zhang, C., 2010. Microbial desulfurization for NR ground rubber by Thiobacillus ferrooxidans. J Appl Polym Sci 116 (5), 2768–2774.

[26] Horikx, M., 1956. Chain scissions in a polymer network. Rubber Chem Technol 29 (4), 1166–1173.

[27] Hu, M., Zhao, S., Li, C., Wang, B., Fu, Y., Wang, Y., 2016. Biodesulfurization of vulcanized rubber by enzymes induced from *Gordonia amicalisa*. Polym Degrad Stab 128, 8–14.

[28] Yao, C., Zhao, S., Wang, Y., Wang, B., Wei, M., Hu, M., 2013. Microbial desulfurization of waste latex rubber with *Alicyclobacillus* sp. Polym Degrad Stab 98 (9), 1724–1730.

[29] Linos, A., Berekaa, M.M., Reichelt, R., Keller, U., Schmitt, J., Flemming, H.C., et al., 2000. Biodegradation of *cis*-1,4-polyisoprene rubbers by distinct actinomycetes: microbial strategies and detailed surface analysis. Appl Environ Microbiol 66 (4), 1639–1645.

[30] Romine, R.A., Romine, M.F., 1998. Rubbercycle: a bioprocess for surface modification of waste tyre rubber. Polym Degrad Stab 59 (1–3), 353–358.

[31] Modrow, H., Hormes, J., Visel, F., Zimmer, R., 2001. Monitoring thermal oxidation of sulfur crosslinks in SBR-elastomers by quantitative analysis of sulfur K-edge XANES-spectra. Rubber Chem Technol 74 (2), 281–294.

[32] Dhez, O., Ade, H., Urquhart, S.G., 2003. Calibrated NEXAFS spectra of some common polymers. J Electron Spectrosc Relat Phenom 128 (1), 85–96.

[33] Li, Y., Zhao, S., Wang, Y., 2011. Microbial desulfurization of ground tire rubber by *Thiobacillus ferrooxidans*. Polym Degrad Stab 96 (9), 1662–1668.

[34] Tsuchii, A., Suzuki, T., Takeda, K., 1985. Microbial degradation of natural rubber vulcanizates. Appl Environ Microbiol 50 (4), 965–970.

[35] Hiessl, S., Böse, D., Oetermann, S., Eggers, J., Pietruszka, J., Steinbüchel, A., 2014. Latex clearing protein-an oxygenase cleaving poly(*cis*-1,4-isoprene) rubber at the *cis* double bonds. Appl Environ Microbiol 80 (17), 5231–5240.

[36] Andler, R., Steinbüchel, A., 2017. A simple, rapid and cost-effective process for production of latex clearing protein to produce oligopolyisoprene molecules. J Biotechnol 241, 184–192.

[37] Nguyen, L.H., Nguyen, H.D., Tran, P.T., Nghiem, T.T., Nguyen, T.T., Dao, V.L., et al., 2020. Biodegradation of natural rubber and deproteinized natural rubber by enrichment bacterial consortia. Biodegradation 31 (4–6), 303–317.

[38] Gao, R., Liu, R., Sun, C., 2022. A marine fungus Alternaria alternata FB1 efficiently degrades polyethylene. J Hazard Mater 431, 128617.

[39] Gao, R., Sun, C., 2021. A marine bacterial community capable of degrading poly (ethylene terephthalate) and polyethylene. J Hazard Mater 416, 125928.

[40] Sato, S., Honda, Y., Kuwahara, M., Watanabe, T., 2003. Degradation of vulcanized and nonvulcanized polyisoprene rubbers by lipid peroxidation catalyzed by oxidative enzymes and transition metals. Biomacromolecules 4 (2), 321–329.

[41] Enoki, M., Doi, Y., Iwata, T., 2003. Oxidative degradation of cis- and trans-1,4-polyisoprenes and vulcanized natural rubber with enzyme-mediator systems. Biomacromolecules 4 (2), 314–320.

[42] Gibu, N., Linh, D.V., Suzuki, N., Thuy Ngan, N.T., Fukuda, M., Anh, T.K., et al., 2022. Identification and transcriptional analysis of poly(cis-1,4-isoprene) degradation gene in *Rhodococcus* sp. strain RDE2. J Biosci Bioeng 133 (5), 452–458.